ISSN 0023-1584, Kinetics and Catalysis, 2008, Vol. 49, No. 1, pp. 68–78. © MAIK "Nauka/Interperiodica" (Russia), 2008.
Original Russian Text © A.V. Krestinin, A.V. Raevskii, M.B. Kislov, G.I. Zvereva, O.I. Kolesova, 2008, published in Kinetika i Kataliz, 2008, Vol. 49, No. 1, pp. 74–84.

Kinetics of Growth of Carbon Fibers on an Iron Catalyst in Methane Pyrolysis: A Measurement Procedure with the Use of an Optical Microscope

A. V. Krestinin, A. V. Raevskii, M. B. Kislov, G. I. Zvereva, and O. I. Kolesova

Institute of Problems of Chemical Physics, Russian Academy of Sciences, Chernogolovka, Moscow oblast, 142432 Russia
E-mail: kresti@icp.ac.ru

Received September 27, 2006

Abstract—A procedure was developed for measuring the kinetic parameters of growth of carbon fibers in the catalytic pyrolysis of hydrocarbons. In this procedure, the dependence of the averaged length of grown fibers on growth time is constructed based on the measurements of fiber lengths with an optical microscope. The procedure proposed allowed us to reliably determine the Arrhenius parameters of the rate of fiber growth and the induction period of fiber nucleation in the measurement of carbon fibers 100 nm or more in diameter. The kinetics of growth of carbon fibers from methane–hydrogen mixtures on an iron catalyst was measured over a temperature range of 950–1050°C. It was found that the rate of fiber growth as a function of methane activity in the gas phase exhibited a maximum in the activity range 200–300; the value of this maximum depends on the contribution of the products of gas-phase methane pyrolysis to the growth of fibers. It was also found that the rate of fiber growth dramatically increased as the critical concentration of pyrolysis products in the mixture was reached. This increase was interpreted as a change from one growth mechanism (growth from methane) to another growth mechanism (growth from acetylene). The experimental data explained the high sensitivity of the process of carbon fiber growth from methane to temperature and the residence time of the gas in the reactor.

DOI: 10.1134/S0023158408010096

INTRODUCTION

The formation of carbon nanofibers/nanotubes in the pyrolysis of hydrocarbons and in the disproportionation of CO has been very intensively studied in the last few years because carbon nanotubes belong to a new class of materials, which is of interest in many applications [1, 2]. Evidently, applied studies on the mechanism of formation of carbon nanostructures are oriented to find efficient and inexpensive processes for the large-scale production of these structures and methods for controlling the growth and structure of nanofibers. This is required for the manufacture of products based on these nanofibers, such as cold emitters, gas-separating membranes, catalyst supports, and filtering layers. These reasons offered the main incentive to study systematically the kinetics of growth of carbon nanofibers. Baker and Harris [3] pioneered such studies more than three decades ago; more recently, other researchers have continued these studies.

Initially, controlled-atmosphere transmission electron microscopy (TEM) was specially developed as a technique for studying the kinetics of growth of carbon nanofibers [3]. In this case, carbon fibers were in situ grown immediately in the chamber of a specially designed electron microscope. The micrographs of a growing fiber successively taken in time allow one to plot the length of the fiber as a function of growth time and hence to determine the rate of fiber growth. An advantage of this technique is that the kinetics of formation of catalytic carbon is measured on a separate catalyst particle. This provides an opportunity to study the dynamics of catalyst poisoning and the effect of the state of a catalyst on its chemical activity. Figure 1 shows a typical curve of fiber growth. This curve can be characterized by the following three numerical parameters: the induction time (τ), the quasi-steady-state growth rate (w), and the maximum length (l_{max}) of a fiber grown under given conditions. All of the above values were found to depend on the type of the catalyst, the temperature, the composition of the gas atmosphere, and the diameter of the growing fiber. Based on these studies, Baker et al. [4, 5] were the first to formulate a model for the growth of a carbon fiber in the simplest case when a catalyst particle is arranged at the head of the growing fiber. This model with refinements still remains commonly accepted. It implies that the chemisorption and dehydrogenation of the parent hydrocarbon molecule occurs at the frontal surface of a catalyst particle followed by the dissolution of carbon in the surface metal layer. Then, the dissolved carbon diffuses to the backside of the particle, where it is released as graphene layers that form the carbon fiber. It follows from the Baker model that good catalysts for the growth of carbon fibers should exhibit a high solubility of carbon and a high diffusion coefficient of dis-

solved carbon in the catalyst material. All of the known catalysts meet these requirements.

The main disadvantage of controlled-atmosphere TEM is that it is labor intensive and requires the use of highly expensive specially designed instrumentation. Therefore, attempts to develop less expensive techniques for kinetic measurements have been made. Currently, a relatively simple gravimetric method is widely used for studying the kinetics of formation of carbon fibers. In this case, changes in the weight of a sample are continuously measured in the course of catalytic pyrolysis. This is performed either by direct weight measurements (for this purpose, a sample with a catalyst is arranged on a microbalance) or indirectly (based on the balance of carbon released on the catalyst) by analyzing the composition of gases at the reactor outlet. This procedure is most simply implemented in the cases of the catalytic disproportionation of carbon monoxide [6] and the pyrolysis of methane at moderate temperatures [7, 8].

The time dependence of the sample weight represents the total rate of growth of carbon fibers with different diameters and includes a number of differently directed side contributions due to the deactivation and fragmentation of catalytic species (e.g., see [6, 9, 10]). The kinetics of these processes depends on the state of the catalyst, the size of catalyst particles, the temperature, and the composition of the gas atmosphere. Audier et al. [10] found that the application of gravimetric data to studying the mechanism of growth of carbon fibers requires a critical analysis of these data. Moreover, with the use of a microbalance, gravimetry is bounded above by a temperature of ~800°C because of technical difficulties in sample weighing in the reaction atmosphere.

In this paper, we describe a procedure developed for the determination of the main parameters of the growth curve for carbon fibers, which is shown in Fig. 1. In this procedure, averaged fiber lengths are measured as functions of growth time. For this purpose, we used an optical microscope in place of an electron microscope; this made the procedure much simpler and less expensive. In addition, statistical measurement data were simultaneously accumulated in order to determine the maximum length of fibers grown under specified conditions. The procedure was simplified by sacrificing the limitation on the diameter of carbon fibers the kinetics of growth of which can be measured (~100 nm and higher). The process of fiber growth was performed separately in an isothermal flow reactor; this retained all limitations on the process parameters of catalytic pyrolysis, including limitations on temperature. The application of the procedure was exemplified in the measurement of the rate of growth of carbon fibers from methane and its mixtures with hydrogen at elevated temperatures (950–1050°C). In this temperature region, the kinetic measurements of carbon fiber growth have almost not been performed, except for scanty data published by Trimm [11].

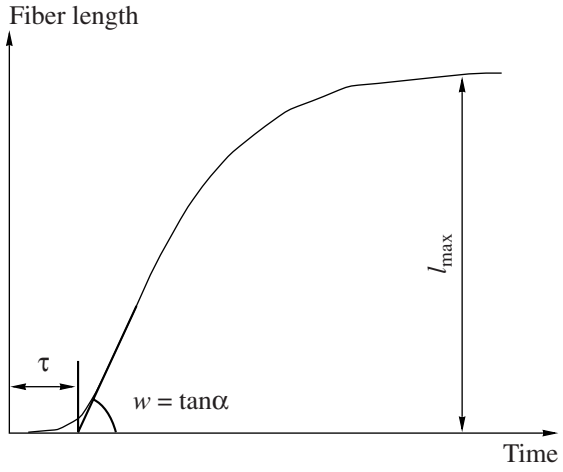

Fig. 1. Typical curve for the growth of a carbon fiber. τ is the time taken to reach the quasi-steady-state rate of growth; w is the rate of the linear growth of a fiber at the quasi-steady-state step of the process; l_{max} is the maximum length of the grown fiber.

It is desirable to know the kinetics of growth of carbon fibers at temperatures from 900 to 1200°C for a few reasons. First, the best results in the synthesis of single-layer carbon nanotubes with supported catalysts were obtained in the above temperature range [12, 13]. Second, we found that special-type carbon nanofibers several millimeters in length can be grown under certain conditions at a rate of 5–10 μm/s in the specified temperature range [14, 15]. The kinetics of growth of ordinary catalytic fibers under these conditions should be known in order to clarify the mechanism of formation of the above fibers.

EXPERIMENTAL

An isothermal flow reactor as a quartz tube 18 mm in i.d. was used to grow carbon fibers. The central portion of the tube was arranged in an electric furnace, the length of the isothermal zone of which was 8 cm. The temperature in the isothermal zone was controlled with an accuracy of ±10°C. A quartz boat with flat substrate plates with a supported catalyst were placed at the center of the isothermal reactor zone. We used iron nitrate and iron oxalate salt microparticles as catalyst precursors. These microparticles were supported by sputtering a solution or evaporating a thin film of the solution from the hot surface of the substrate. Fused quartz plates were used as substrates; this allowed us to perform observations in transmitted and reflected unpolarized or polarized light. A substrate with a catalyst was placed in the reactor and heated to the required temperature (950–1050°C) in a flow of argon. A broad particle-size distribution of iron oxides (from hundredths of a micrometer to ten micrometers) resulted from the decomposition of salts on the substrate in the course of heating the sample. Then, a mixture of methane with

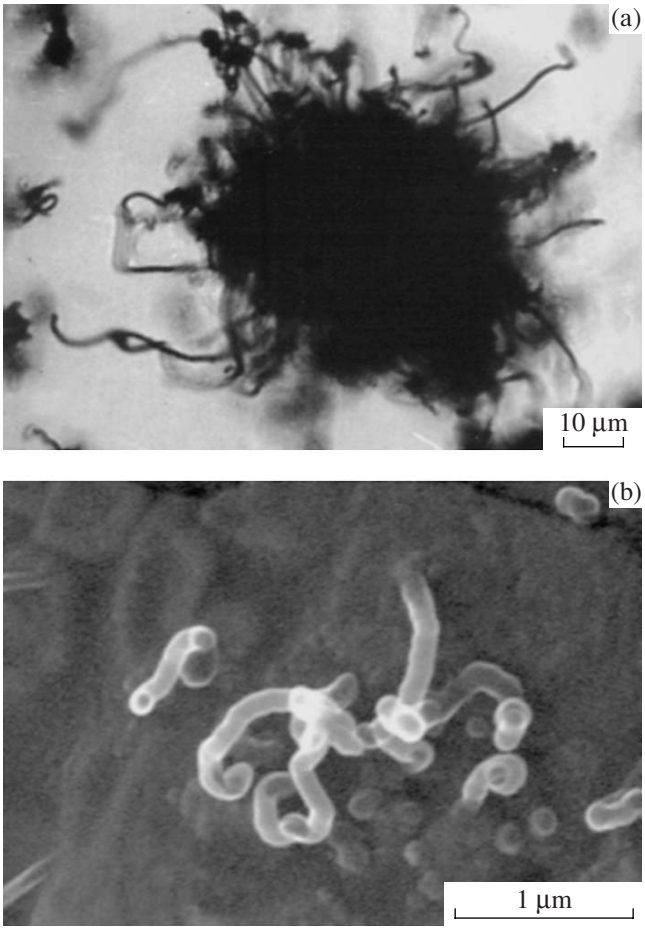

Fig. 2. (a) Optical micrograph of carbon fibers grown on an iron catalyst. Substrate: quartz plate. (b) Scanning electron micrograph of carbon fibers of the same type.

hydrogen in a specified proportion (10–100% CH_4/H_2) was passed through the reactor at a specified flow rate (0.3–1.2 l/min) for a specified time (usually, between 3 and 30 min). The reduction of oxides and the formation of catalytic iron particles occurred directly under conditions of carbon fiber growth after the introduction of the CH_4/H_2 mixture into the reactor. Thus, in our case, the induction period or the time from the onset of the process to the attainment of the quasi-equilibrium rate of fiber growth included the reduction of the catalyst from an oxide species and the formation of the carbon fiber nucleus. The process of fiber growth was terminated after a given time by pumping the reaction mixture from the reactor with a backing pump followed by cooling the reactor to room temperature in a flow of argon. The substrate was removed and analyzed by optical microscopy. Chemically pure methane (Balashikha Oxygen Works; methane, ≥99.9%; oxygen + nitrogen, ≤0.07%; ethane + propane, ≤0.03%; water vapor, ≤0.004%), which was additionally purified by passing the working mixture through a zeolite bed (NaA zeolite, OOO Real Sorb) at room temperature, was used in the experiments. We found in preliminary experiments that the results obtained with the use of the additional purification and without it were dramatically different. This fact is indicative of the considerable effect of minor impurities in a methane–hydrogen mixture on the kinetics of the process. According to mass-spectrometric data, water and, probably, propane comprised the main amount of impurities absorbed by the zeolite.

At a length of several micrometers or more, carbon fibers are clearly visible in an optical microscope even if their diameter is no higher than 50–100 nm; that is, it lies in a nanosized region. We managed to measure the length of fibers from a few micrometers to several millimeters because of a broad visual field and the possibility of micrometric measurements in an optical microscope. Figure 2 shows an optical micrograph of a typical sample of carbon fibers grown from methane on a quartz substrate with supported iron oxalate particles. It can be seen that individual fibers or their parts have fuzzy edges because of the small depth of focus in the optical microscope. It is easy to trace an individual fiber along the full length and simultaneously determine the spatial arrangement of its parts by changing the focusing of the microscope. Unlike an optical microscope, fibers in a micrograph taken with a scanning electron microscope appear sharper (Fig. 2b). However, it is practically impossible to restore their spatial arrangement; because of this, the length of the fibers is difficult to measure accurately.

The procedure for the determination of the kinetic parameters of fiber growth and nucleation consisted in the following: A series of experiments was performed to grow fibers on substrates with an identically supported catalyst at the same temperature and gas atmosphere composition. In the experiments, the time of growth was chosen so that the determined lengths of carbon fibers linearly increased with experiment time. This linear dependence suggested that the measurements were performed in the quasi-steady-state (linear) section of fiber growth. The length of fibers was determined by measuring the longest fibers in 15 fields with an area of $240 \times 360\ \mu m^2$, which were randomly chosen in each particular sample of size 10 mm × 10 mm, followed by averaging these data over the measured array. Fibers with approximately equal diameters (~0.1 μm) were chosen for the measurements, unless otherwise specified. Table 1 and Fig. 3 show the averaged fiber lengths for several typical experimental conditions (temperature and mixture composition). Graphs in Fig. 3 show that a linear relationship between the averaged fiber length and the experiment time was obeyed. Note that each experimental point in Fig. 3 was obtained in different experiments with different times of fiber growth. The accuracy of the measurement of growth time depended on the duration of transient processes (filling the reactor with the reaction atmosphere and evacuation) and was estimated at ±10 s. For an experiment temperature of 1000°C, the root-mean-square deviations of the measured data array from aver-

Table 1. Averaged lengths (l) of carbon fibers depending on growth conditions

30% CH_4/H_2				50% CH_4/H_2			
	950°C	1000°C	1050°C		950°C	1000°C	1050°C
Δt, min*	l, μm			Δt, min	l, μm		
5	–	–	6.6	5	–	–	6.0
10	1.6	3.9	13.75	10	0.3	5.8	16.4
15	–	–	19.33	15	–	–	26.1
20	2.8	8.9	–	20	5.2	16.2	–
30	5.0	13.1	–	30	9.8	24.4	–
70% CH_4/H_2				100% CH_4			
	950°C	1000°C	1050°C		950°C	1000°C	1050°C
Δt, min	l, μm			Δt, min	l, μm		
5	–	–	2.5	5	–	–	3.4
7.5	–	–	–	7.5	–	–	10.8
10	3.4	4.4	–	10	0.9	2.7	17.3
15	–	–	10.3	15	–	–	–
20	6.9	11.0	–	20	1.0	5.7	–
30	11.8	17.8	22.0	30	2.1	10.1	–

* Δt is the duration of growth.

age values are shown; usually, they amounted to ~10% of the average fiber length. The rates of fiber growth were determined from the slopes of straight lines that approximated experimental data. The duration of the induction period in the formation of fibers under given conditions was determined by extrapolating these straight lines to the axis of time (to the zero length of fibers).

RESULTS

Table 2 summarizes the rates of fiber growth determined under various experimental conditions and their Arrhenius approximations, which are also graphically shown in Fig. 4. These graphs indicate that the Arrhenius equations remained linear over the temperature range 950–1050°C for all of the mixture compositions except for pure methane. Thus, the procedure used in this study allowed us to determine reliably the activation energy of carbon fiber growth. For pure methane, the activation energy exhibited a pronounced temperature dependence. The reasons for this phenomenon will be considered below. Table 3 and Fig. 5 summarize data on the duration of the induction period before the onset of fiber growth. Again, the activation energy remained a weakly changing value in this temperature segment at a constant gas phase composition.

Figure 6 shows the dependence of the rate of growth of carbon fibers on the concentration of methane at various temperatures. However, we found in the subsequent experiments that the concentration of methane in the initial mixture cannot serve as an unambiguous characteristic of the gas phase for the growth of carbon fibers at elevated temperatures. This is indicated by data on changes in the rate of fiber growth upon varying the flow rate of the gas mixture, which are shown in Fig. 7.

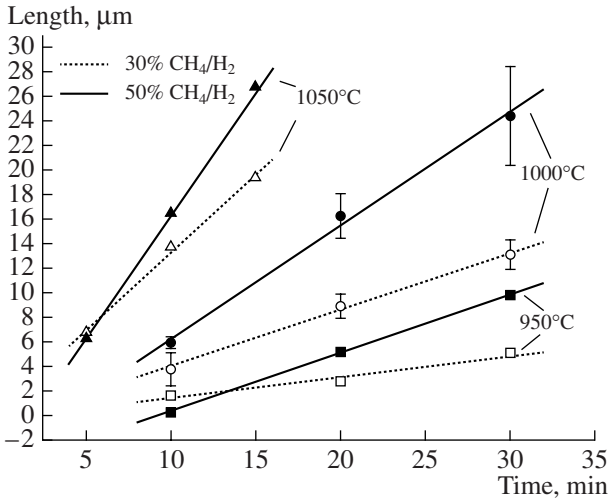

Fig. 3. Dependence of the average length of carbon fibers on experiment time. Catalyst: iron. Gas supply rate v = 0.6 l/min.

Table 2. Rate of growth (w) of carbon fibers depending on experimental conditions

T, °C	$a^*_{C(gas)}$	w, nm/s	T, °C	$a^*_{C(gas)}$	w, nm/s
30%CH_4/H_2			50%CH_4/H_2		
950	42.2	2.8	950	138	7.9
1000	58.3	7.8	1000	191	15
1050	80.3	21	1050	262	33
$w = 7.9 \times 10^{11}\exp(-270000/RT)$**			$w = 1.5 \times 10^{9}\exp(-195000/RT)$**		
T, °C	$a^*_{C(gas)}$	w, nm/s	T, °C	$a^*_{C(gas)}$	w, nm/s
70%CH_4/H_2			100%CH_4		
950	536	7.7	950	∞	1.0
1000	741	11	1000	∞	6.2
1050	1020	13	1020	∞	46
$w = 3.1 \times 10^{4}\exp(-84000/RT)$**			$w = 2.7 \times 10^{28}\exp(-671000/RT)$**		

* The activity of gas-phase (methane) carbon was calculated for the equilibrium constant $K_{CH_4} = 4.5 \times 10^5\exp(-90123/RT)$ (J, mol, K) [21].

** Activation energy in J/mol.

It can be seen that the lower the rate of gas supply, that is, the longer the average residence time of the gas in the reactor, the higher the rate of fiber growth. It is clear that the change of the rate of growth can be explained by the change of the composition of the gas phase due to gas-phase reactions. On the other hand, we found that, in our case, the rate of growth was practically independent of catalyst particle size over the range 0.1–0.3 μm.

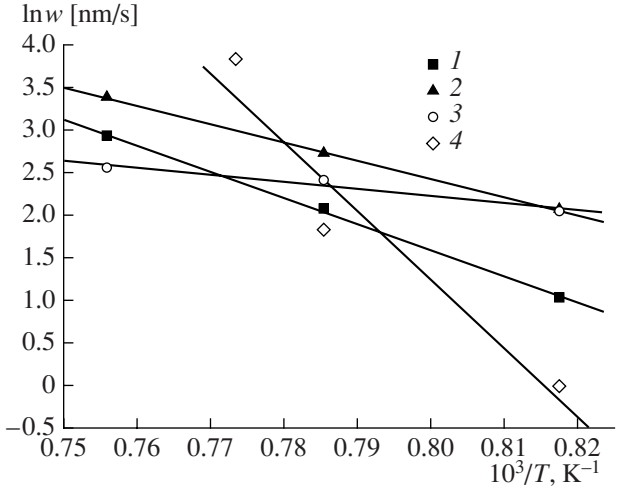

Fig. 4. Rate of growth of carbon fibers from CH_4–H_2 mixtures of different compositions in Arrhenius coordinates: (*1*) 30% CH_4–H_2, E_a = 270 kJ/mol; (*2*) 50% CH_4–H_2, E_a = 195 kJ/mol; (*3*) 70% CH_4–H_2, E_a = 84 kJ/mol; (*4*) 100% CH_4–H_2, E_a = 671 kJ/mol. Gas supply rate v = 0.6 l/min.

Because we used quartz as a substrate and iron oxide as a catalyst precursor in our experiments, we cannot a priori exclude the possibility of the partial introduction of silicon into the catalytic particle and the effect of silicon on the diffusion of carbon. Our control experiments on the growth of carbon fibers on quartz and sapphire substrates under identical conditions demonstrated that the average lengths of carbon fibers were equal to within ±(2–3)% in both cases; that is, they lay within the limits of experimental error. Thus, the contamination of the catalyst by a silicon impurity and the effect of the substrate on the kinetic data were excluded.

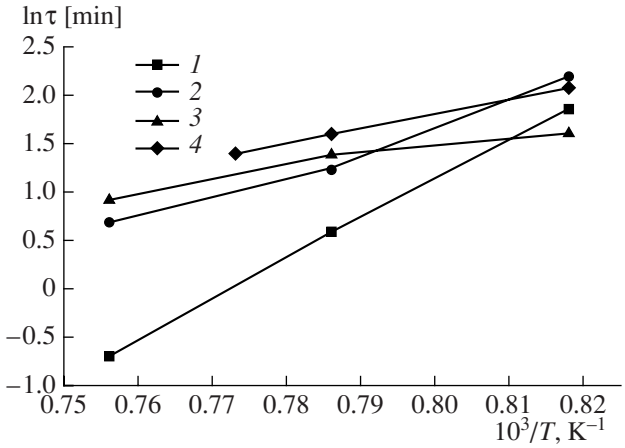

Fig. 5. The temperature dependence of the induction period before the onset of growth of carbon fibers in Arrhenius coordinates at various gas compositions: (*1*) 30, (*2*) 50, (*3*) 70, and (*4*) 100% CH_4. Gas supply rate v = 0.6 l/min.

Table 3. Induction period (τ) before the onset of growth of carbon fibers depending on experimental conditions

T, °C	$a^*_{C(gas)}$	τ, s	T, °C	$a^*_{C(gas)}$	τ, s
30%CH_4/H_2			50%CH_4/H_2		
950	42.2	390	950	138	540
1000	58.3	110	1000	191	210
1050	80.3	30	1050	262	120
$\tau = 7.5 \times 10^{-13}\exp(347000/RT)$**			$\tau = 1.2 \times 10^{-6}\exp(202000/RT)$**		
T, °C	$a^*_{C(gas)}$	τ, s	T, °C	$a^*_{C(gas)}$	τ, s
70%CH_4/H_2			100%CH_4		
950	536	300	950	∞	480
1000	741	240	1000	∞	300
1050	1020	150	1020	∞	240
$\tau = 3.5 \times 10^{-2}\exp(93000/RT)$**			$\tau = 1.6 \times 10^{-3}\exp(129000/RT)$**		

* The activity of gas-phase (methane) carbon was calculated for the equilibrium constant $K_{CH_4} = 4.5 \times 10^5\exp(-90123/RT)$ (J, mol, K) [21].

** Activation energy in J/mol.

DISCUSSION

Here, we shall restrict our consideration to an analysis of the dependence of the quasi-steady-state rate of growth of carbon fibers on an iron catalyst upon process parameters. Tables 1 and 2 and Figs. 3, 4, 6, and 7 summarize the initial kinetic data. The temperature and gas phase composition are the main process parameters responsible for the quasi-steady-state rate of growth of fibers under conditions of our experiments.

From the standpoint of nonequilibrium thermodynamics [16, 17], the growth of a carbon fiber (at the step of quasi-steady-state growth) should be considered as the stable nonequilibrium state of the catalytic particle on which the fiber grows. Two special features of the formation of these nonequilibrium states, which are referred to as dissipative structures, are well known. These are the nonlinearity of the internal dynamics of the process and the supercritical values of the external parameters of the system; in the case under discussion, these parameters determine the states of the gas phase and carbon fiber material. Usually, the activity of gas-phase carbon ($a_{C(gas)}$) is used as a parameter that characterizes the deviation of external conditions or surroundings from thermodynamic equilibrium. By defini-

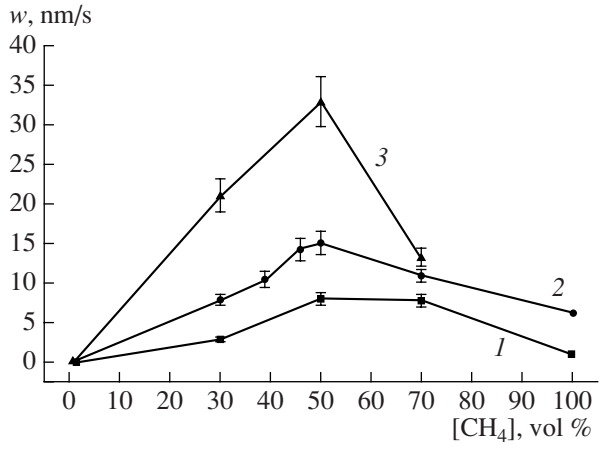

Fig. 6. Dependence of the rate of growth of carbon fibers on the methane concentration in the starting mixture at various experimental temperatures: (*1*) 950, (*2*) 1000, and (*3*) 1050°C. Gas supply rate $v = 0.6$ l/min.

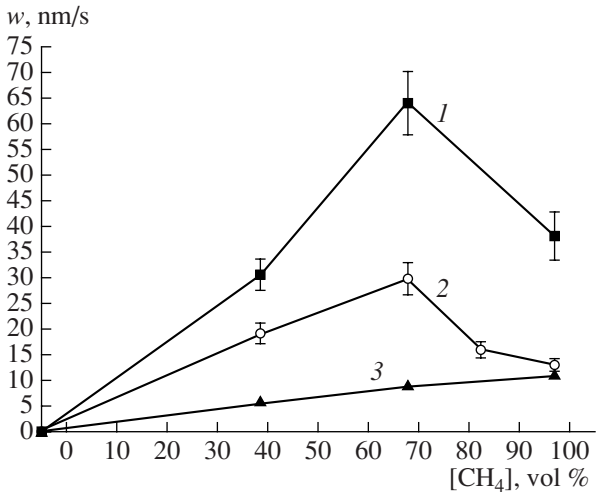

Fig. 7. Dependence of the rate of growth of carbon fibers on the methane concentration in the starting mixture at T = 1050°C and the gas supply rates v = (*1*) 0.3, (*2*) 0.6, and (*3*) 1.2 l/min.

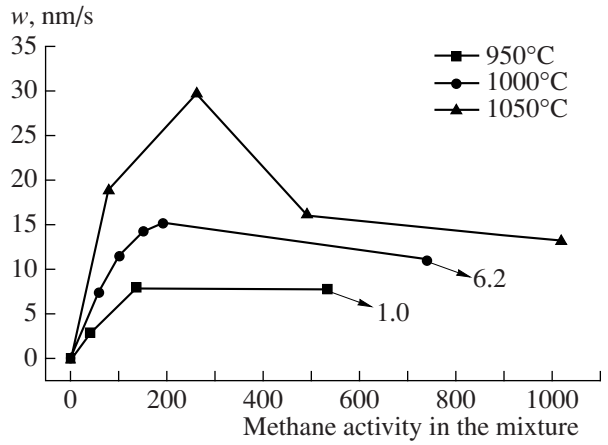

Fig. 8. Rate of growth of carbon fibers as a function of the methane activity in the starting mixture. Arrows with numbers refer to the rates of fiber growth in an atmosphere of pure methane ($a_{C(gas)} \longrightarrow \infty$). Gas supply rate v = 0.6 l/min.

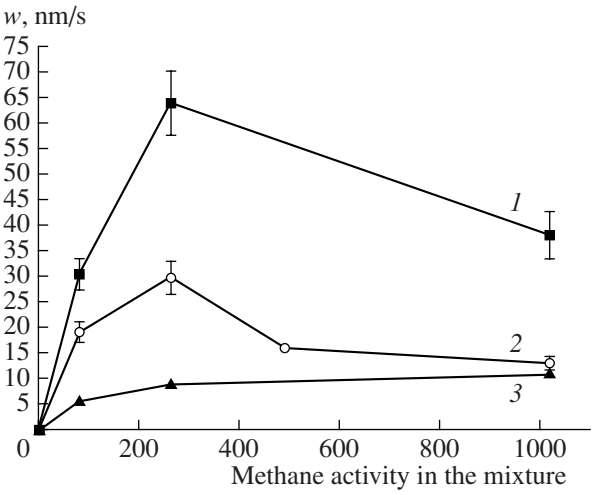

Fig. 9. Rate of growth of carbon fibers at T = 1050°C as a function of the methane activity in the starting mixture at the gas supply rates v = (*1*) 0.3, (*2*) 0.6, and (*3*) 1.2 l/min.

tion, $a_{C(gas)}$ is the ratio of the fugacity of carbon in the gas atmosphere to the fugacity of carbon in the standard state (graphite) at the same temperature. For a mixture of a hydrocarbon C_nH_m with hydrogen, the activity of carbon in the gas phase is calculated as follows:

$$a_{C(gas)} = [(P_{C_nH_m})^{1/n}]K_{C_nH_m}/[P_{H_2}]^{m/2n}. \quad (1)$$

Here, $P_{C_nH_m}$ and P_{H_2} are the partial pressures of the hydrocarbon and hydrogen, respectively, in the gas referenced to a standard value (1 bar); $K_{C_nH_m}$ is the equilibrium constant of the reaction of hydrocarbon thermodecay to graphite and hydrogen

$$(1/n)C_nH_m = C(\text{graphite}) + (m/2n)H_2. \quad (I)$$

The difference between two values that determine the activity of carbon in the gas phase and the activity of carbon in a carbon fiber ($a_{C(fiber)}$), $\Delta a = (a_{C(gas)} - a_{C(fiber)})$, is a measure of the deviation of the external parameters of the system from thermodynamic equilibrium. The value of $a_{C(fiber)}$ is equal to the fugacity of carbon in the fiber, and it is defined as the equilibrium constant K_{fiber} of the reaction

$$C(\text{fiber}) = C(\text{graphite}). \quad (II)$$

The excess free Gibbs energy for a carbon fiber with reference to graphite, which is responsible for the value of K_{fiber}, depends on many factors (the morphology and structure of the fiber, the composition of the fiber-forming material (for example, the amount of hydrogen in it), the density of defects in the material, the fiber diameter, etc.), which remain to be identified accurately. The free Gibbs energy and the enthalpy of formation of carbon fibers/tubes decrease with diameter. Alstrup [18] experimentally found that $\Delta G_f \cong$ 7–8 kJ/mol and $\Delta H_f \cong$ 15 kJ/mol for carbon nanofibers ~20 nm in diameter at T = 500°C. By this is meant that the activity of carbon $a_{C(fiber)} < 2$–3 at 1000°C. According to data published by Peigney et al. [19], the threshold concentration of methane in hydrogen at which the formation of single-layer nanotubes comes into play at T = 1050°C is 1.5%, which is also consistent with the value $a_{C(fiber)} \cong 2$.

The generalized thermodynamic force in the system, which tends to bring the system to chemical equilibrium, is expressed in terms of the activities of carbon in the gas phase and a carbon fiber as follows:

$$X_{chem} = -\Delta G_r/RT = \ln(a_{C(gas)}/a_{C(fiber)}), \quad (2)$$

where ΔG_r is the change of the free Gibbs energy in the reaction of carbon fiber formation

$$(1/n)C_nH_m = C(\text{fiber}) + (m/2n)H_2. \quad (III)$$

It is convenient to use the coordinate Δa for measuring the deviation of the external parameters of the system from equilibrium because Δa defines the concentration gradient of dissolved carbon in a catalytic particle and the rate of growth of a carbon fiber in the case that diffusion is a growth-limiting factor and the value of Δa is sufficiently small [20].

Figures 8 and 9 show the above primary data on the quasi-steady-state rates of fiber growth as functions of the activity of carbon in methane, which was calculated from Eq. (1). The equilibrium constant K_{CH_4} was taken from [21]:

$$K_{CH_4} = 4.5 \times 10^5 \exp(-90123/RT) \text{ (J, K)}.$$

In the graphs, the rates of fiber growth were extrapolated to zero for $a_{C(gas)} = 1$. All of the graphs in Figs. 8 and 9 have a number of common features:

(a) there is an approximately linear initial portion in the dependence of the rate of growth on the activity of

carbon; this initial portion is not beyond the scope of $a_{C(gas)} \approx 50$;

(b) the rate of fiber growth reaches a maximum in the range $a_{C(gas)} \approx 200–300$, and this maximum becomes clearer as the temperature is increased and the rate of gas supply is decreased;

(c) the rate of fiber growth practically does not exhibit a maximum at high rates of gas supply (Fig. 9, 1.2 l/min);

(d) the rate of growth monotonically decreases at high activities of methane.

Audier and Coulon [22] were the first to measure the dependence of the rate of carbon fiber weight growth on the activity of carbon in CH_4/H_2 and CO/CO_2 mixtures by gravimetry up to $a_{C(gas)} \approx 10–15$ ($T = 500–650$°C). It was found that the rate of growth of fibrous carbon was proportional to the activity of carbon at low activities of gas-phase carbon. More recently, Bianchini and Lund [7] also used gravimetry to measure the dependence of the rate of growth of fibrous carbon over the entire range of carbon activities ($T = 600–800$°C). At low carbon activities (to $a_{C(gas)} \approx 20–30$), they also obtained the linear dependence of the rate of growth on the activity. At high carbon activities, the rate of growth remained almost constant. Thus, the graphs of the rate of fibrous carbon weight growth obtained by Bianchini and Lund [7] are identical in shape to the graph of the rate of growth of the individual carbon fiber shown in Fig. 9 for a gas supply rate of 1.2 l/min.

A special feature of the experimental procedure used by Bianchini and Lund [7] was that a heated tube reactor was incorporated into the gas circulation circuit. Initially, the closed circuit was filled with pure methane; as methane was consumed in the catalytic pyrolysis reaction, it was converted into a mixture of methane with hydrogen. In this case, the rate of fibrous carbon weight growth was measured at various methane concentrations as the gas composition changed in the same experiment with the same catalyst sample. Thus, the rates of growth at various activities of gas-phase carbon were measured on a catalyst whose state uncontrollably changed from one measurement to another. It is likely that for this reason Bianchini and Lund [7] failed to obtain the temperature dependence of the rate of weight growth of fibrous carbon. Moreover, some points in the graphs exhibited local maximums of the rate of growth (e.g., Fig. 5, 913 K, $a_{C(gas)} = 256$ [7]), and they were rejected in interpretation of the experimental data.

It will be demonstrated below that the occurrence of a maximum of the rate of carbon growth as a function of carbon activity was primarily due to the gas-phase reactions of methane pyrolysis and the contribution of methane pyrolysis products to the growth of fibers. Hence, it would be expected that, in pure methane–hydrogen mixtures, the graph of the dependence of the rate of growth on the activity of methane has the shape of the curve shown in Fig. 9 for a flow rate of 1.2 l/min. Nevertheless, it is most likely that the rate of growth in pure methane–hydrogen mixtures exhibits a weakly pronounced maximum. This is indicated by the measurements of the rate of formation of fibrous carbon from methane performed by Snoeck et al. [8], who used gravimetry ($T = 580–680$°C), as well as Bianchini and Lund [7]. Unlike the published data in [7], Snoeck et al. [8] observed a pronounced local maximum of the rate of growth as a function of the partial pressure of hydrogen at a constant methane pressure of 1.5 bar (Figs. 2, 3 in [8]). The growth rate maximum disappeared only as the pressure of methane was increased to 5 and 10 bar; Snoeck et al. [8] explained this fact by the limiting effect of diffusion in a gas at elevated pressures. Snoeck et al. [8] also measured the equilibrium constant of the reaction of carbon fiber formation from methane in the temperature range 580–680°C; this also suggests a sufficiently high accuracy of measurements. In our experiments, we failed to answer unambiguously the question of the occurrence of a maximum of the rate of fiber growth in pure methane–hydrogen mixtures because carbon fibers practically did not grow in these mixtures at $T = 950$°C or higher. As a result, we failed to collect sufficient statistical data for reliable measurement of the rate of growth.

The increase of the rate of growth of carbon fibers by a factor of tens as the rate of gas supply was decreased from 1.2 to 0.3 l/min (Fig. 9) clearly indicates that only an increased contribution of methane pyrolysis products to the growth of fibers can be responsible for the above phenomenon. It is well known that, at temperatures higher than 1000°C, the gas-phase pyrolysis of methane is accelerated so that methane decomposition products (primarily, ethylene and acetylene) have a chance to accumulate in detectable amounts in the gas atmosphere if the gas residence time in the reactor is ~1 s or longer. The average residence time of a gas in the isothermal zone of our reactor (τ_{gas}) was calculated from the equation

$$\tau_{gas} = V_r T_{room}/(v T_r),$$

where V_r is the volume of the isothermal zone of the reactor (l), v is the rate of gas supply (l/min), and T_{room} and T_r are room temperature and the temperature in the isothermal zone of the reactor (K). In our case, the average residence times of a gas were 0.90, 0.45, and 0.22 s at gas supply rates of 0.3, 0.6, and 1.2 l/min, respectively.

In the case of a gas atmosphere composed of a mixture of various hydrocarbons in chemical equilibrium with each other, there is a single value of carbon activity in the gas phase, $a_{C(gas)}$, which is calculated from Eq. (1). Any equilibrium component in this system can be taken for calculations. However, the activities of carbon in various hydrocarbons are different if chemical equilibrium is absent from the gas phase. Figure 10 shows the results of the calculation of the kinetics of gas-phase pyrolysis of a 50% CH_4/H_2 mixture at $T = 1050$°C. This calculation was performed with the use of a detailed reaction scheme, which was applied previ-

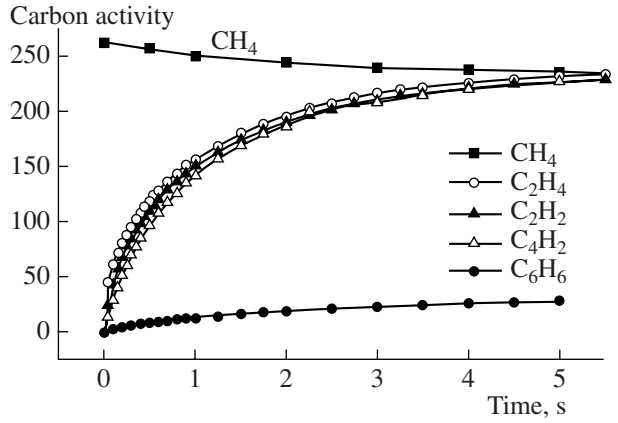

Fig. 10. Calculated changes in the activity of carbon in particular gas-phase components as functions of the time of pyrolysis at T = 1050°C. Starting mixture: 50% CH_4/H_2.

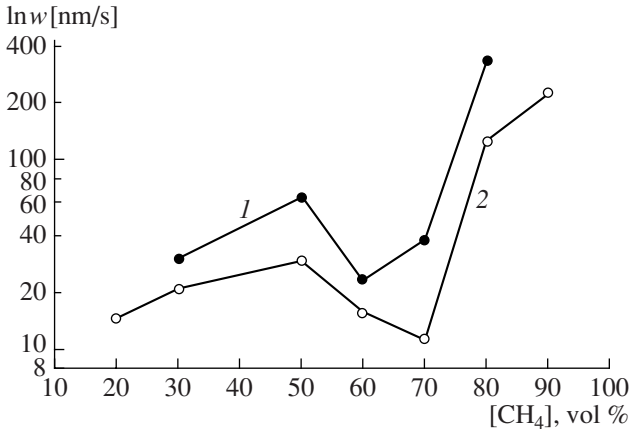

Fig. 11. Dependence of the rate of growth of carbon fibers on the concentration of methane in the mixture at T = 1050°C and the gas supply rates v = (*1*) 0.3 and (*2*) 0.6 l/min.

ously to study the kinetics of formation of soot particles from hydrocarbons [23, 24]. The main products of methane pyrolysis in the gas phase are ethylene and acetylene, whose concentrations are represented as the corresponding activities of carbon calculated from Eq. (1). In Fig. 10, it can be seen that a gas-phase chemical equilibrium for primary pyrolysis products (ethylene and acetylene) was established in a time of ~3–5 s. The absolute concentrations of the main gas-phase components in equilibrium were as follows: methane, 47.5 vol %; ethylene, 0.41 vol %; acetylene, 0.41 vol %. After the accumulation of acetylene in the gas phase, two main molecular families (polyyne and polyaromatic) began to form with the participation of acetylene. Both of the families are thermodynamically most stable under the specified conditions [25]. The concentrations of polyynes much more rapidly reached their equilibrium values, as compared with polyaromatic molecules, which were formed noticeably more slowly in a multistep chemical process. As can be seen in Fig. 10, the activity of carbon in diacetylene increased somewhat more slowly than the activity of carbon in acetylene. At the same time, the activity of carbon in benzene (the simplest aromatic molecule) remained lower than the activity of carbon in acetylene by a factor of tens. Finally, as the gas-phase equilibrium is reached, the activities of carbon for all of the gas-phase components approach the same value.

A remarkable feature of the growth of carbon fibers in methane–hydrogen mixtures (at temperatures to ~1000–1100°C) is that the equilibrium concentrations of methane pyrolysis products in these mixtures are lower than the concentration of methane by a factor of tens [26]. As a result of this, the activity of methane remains almost constant in the course of gas-phase chemical equilibration for small hydrocarbons. Thus, the activity of methane in the starting mixture can be used for the quantitative expression of the deviation of the external parameters of the system from equilibrium conditions rather than for the complete characterization of the chemical composition of the gas atmosphere.

As follows from Fig. 10, for the residence times of a gas in the reactor under the conditions of our experiments (τ_{gas} = 0.2–0.9 s), the activity of carbon in ethylene, acetylene, and diacetylene considerably increased and approached the activity of carbon in methane for a gas supply rate of 0.3 l/min. In other pyrolysis products, the activity of carbon remained noticeably lower; therefore, their contribution to the growth of fibers at short residence times of the gas in the reactor can be ignored. Indeed, as can be seen in Fig. 9, the contribution of a particular hydrocarbon to the growth of a fiber essentially depends on its chemical nature. For example, we found by calculations that, at the concentrations of ethylene (~0.1%), acetylene (~0.1%), and diacetylene (~0.0003%) in the gas phase lower than the concentration of methane by a factor of hundreds, the contributions of these hydrocarbons to the rate of fiber growth become higher than the contribution of methane.

The considerable contribution of methane pyrolysis products to the growth of carbon fibers explains the strong dependence of the apparent activation energy of the rate of growth on the concentration of methane in the starting mixture, which was observed in our experiments (Table 2). Indeed, at low methane concentrations in hydrogen, the concentrations of methane pyrolysis products in the gas phase considerably increased with temperature. Thus, the range of changes in the rate of fiber growth in the temperature interval 950–1050°C was increased and, correspondingly, the apparent activation energy of the rate of growth increased. As the concentration of methane was increased, its pyrolysis products began to participate in the growth of fibers even at the lower limit of the temperature interval, at 950°C. In this case, the range of changes in the rate of growth decreased over the entire temperature interval 950–1050°C. Correspondingly, the apparent activation energy also decreased. The subsequent dramatic

increase in the activation energy of fiber growth at high methane concentrations should be discussed separately.

As can be seen in Fig. 7, the contribution of the products of gas-phase methane pyrolysis to the growth of fibers near the maximum rate of growth (at a ~50% methane concentration in the mixture) is higher than the contribution of methane by a factor of ~10 at a gas supply rate of 0.3 l/min. It is likely that the maximum rate of growth will increase to values characteristic of the growth of carbon fibers from acetylene as the rate of gas supply will be further decreased. The latter value is ~400 nm/s for carbon fibers ~20 nm in diameter [27], and it reaches ~1–2 μm/s in the growth of single-layer carbon nanotubes [28]. Note that both of the values are consistent with each other in terms of the dependence of the rate of growth of a carbon nanofiber/nanotube on the diameter (d) of a catalytic particle: $w \sim d^{-0.5}$ [27]. The question arises of how a change from low rates of growth to high rates occurs as the concentration of methane pyrolysis products in the mixture increases: smoothly or abruptly with a decreasing rate of gas supply?

We failed to perform experiments at low rates of gas supply because of the technical limitations of the experimental setup. However, the contribution of pyrolysis products to the rate of fiber growth can be increased in another way by increasing the concentration of methane in the starting mixture. Figure 11 shows the results of these experiments. It can be seen that the rate of fiber growth initially decreased to a minimum at a ~60–70% concentration of methane in the mixture and then dramatically increased once again over the range of methane concentration changes from 70 to 80%. Indeed, in this case, the rate of growth of carbon fibers was as high as 200–400 nm/s, which is characteristic of the growth of fibers in an atmosphere of acetylene. In terms of nonequilibrium thermodynamics, the result consists in the following: As the concentration of methane pyrolysis products in methane mixtures with hydrogen increases, the stable nonequilibrium state of a catalytic particle (tentatively referred to as the mechanism of growth from methane) changes to another stable nonequilibrium state (tentatively referred to as the mechanism of growth from acetylene). This change occurs abruptly as the critical concentration of pyrolysis products is reached in the methane–hydrogen mixture. This change is responsible for a jump in the apparent activation energy of growth, which is shown in Fig. 4 for pure methane.

In conclusion, note that we were the first to observe specially structured carbon fibers ~0.1 μm in diameter and several millimeters in length on substrates at a 70% methane concentration and gas flow rates of 0.3 and 0.6 l/min; these fibers grew by a noncatalytic growth mechanism (second-type fibers [14]). As the concentration of methane was increased to 80% or higher, these fibers were formed at all of the three gas flow rates: 0.3, 0.6, and 1.2 l/min. The structure of these fibers was described in detail elsewhere [14, 15]. Note that the rate of the catalytic growth of carbon fibers under all of the test conditions of the pyrolysis of methane–hydrogen mixtures was no higher than 0.3–0.4 μm/s and remained much lower than the rate of the noncatalytic growth of carbon fibers, which was as high as 5–10 μm/s [14, 15].

ACKNOWLEDGMENTS

This work was supported in part by the Russian Foundation for Basic Research, project no. 05-03-33119. We are grateful to V.M. Martynenko (Institute of Problems of Chemical Physics, Russian Academy of Sciences) for performing the mass-spectrometric examinations of methane and to V.V. Artemov (Shubnikov Institute of Crystallography, Russian Academy of Sciences) for taking the micrographs of carbon fibers in a scanning electron microscope.

REFERENCES

1. *Nanoengineered Nanofibrous Materials*, Guceri, S., Gogotsi, Yu.G., and Kusnetsov, V., Eds., Dordrecht: Kluwer, 2004.
2. Rakov, E.G., *Usp. Khim.*, 2000, vol. 69, no. 1, p. 41.
3. Baker, R.T.K. and Harris, P.S., *J. Phys. E: Sci. Instrum.*, 1972, vol. 5, no. 8, p. 793.
4. Baker, R.T.K., Barber, M.A., Harris, P.S., Feates, F.S., and Waite, R.J., *J. Catal.*, 1972, vol. 26, p. 51.
5. Baker, R.T.K., Harris, P.S., Thomas, R.B., and Waite, R.J., *J. Catal.*, 1973, vol. 30, p. 86.
6. Audier, M., Coulon, M., and Bonnetain, L., *Carbon*, 1983, vol. 21, no. 2, p. 99.
7. Bianchini, E.C. and Lund, C.R.F., *J. Catal.*, 1989, vol. 117, p. 455.
8. Snoeck, J.-W., Froment, G.F., and Fowles, M., *J. Catal.*, 1997, vol. 169, p. 250.
9. Audier, M., Coulon, M., and Bonnetain, L., *Carbon*, 1983, vol. 21, no. 2, p. 93.
10. Audier, M., Coulon, M., and Bonnetain, L., *Carbon*, 1983, vol. 21, no. 2, p. 105.
11. Trimm, D.L., *Catal. Rev. Sci. Eng.*, 1977, vol. 16, no. 2, p. 155.
12. Peigney, A., Coquay, P., Flahaut, E., Vandenberghe, R.E., de Grave, E., and Laurent, C., *J. Phys. Chem. B*, 2001, vol. 105, p. 9699.
13. Nagy, J.B., Bister, G., Fonseca, A., Mehn, D., Konya, Z., Kiricsi, I., Horvath, Z.E., and Biro, L.P., *J. Nanosci. Nanotechnol.*, 2004, vol. 4, no. 4, p. 326.
14. Krestinin, A.V., Raevskii, A.V., Zhigalina, O.M., Zvereva, G.I., Kislov, M.B., Kolesova, O.I., Artemov, V.V., and Kiselev, N.A., *Kinet. Katal.*, 2006, vol. 47, no. 4, p. 514 [*Kinet. Catal.* (Engl. Transl.), vol. 47, no. 4, p. 497].
15. Kiselev, N.A., Krestinin, A.V., Raevskii, A.V., Zhigalina, O.M., Zvereva, G.I., Kislov, M.B., Artemov, V.V., Grigoriev, Yu.V., and Hatchison, J.L., *Carbon*, 2006, vol. 44, no. 11, p. 2289.
16. Ebeling, W., Engel, A., and Feistel, R., *Physik der Evolutionsprozesse*, Berlin: Akademie, 1990.

17. Parmon, V.N., *Catal. Today*, 1999, vol. 51, nos. 3–4, p. 435.
18. Alstrup, I., *J. Catal.*, 1988, vol. 109, p. 241.
19. Peigney, A., Laurent, Ch., and Rousset, A., *J. Mater. Chem.*, 1999, vol. 9, p. 1167.
20. Holstein, W.L., *J. Catal.*, 1995, vol. 152, p. 42.
21. *Termodinamicheskie svoistva individual'nykh veshchestv: Spravochnik* (Thermodynamic Properties of Individual Compounds: A Handbook), Glushko, V.P., Ed., Moscow: Nauka, 1979, vol. 2.
22. Audier, M. and Coulon, M., *Carbon*, 1985, vol. 23, no. 3, p. 317.
23. Krestinin, A.V., *Khim. Fiz.*, 1998, vol. 17, no. 8, p. 41.
24. Krestinin, A.V., *Combust. Flame*, 2000, vol. 120, p. 513.
25. Krestinin, A.V., Kislov, M.B., Raevskii, A.V., Kolesova, O.I., and Stesik, L.N., *Kinet. Katal.*, 2000, vol. 41, no. 1, p. 102 [*Kinet. Catal.* (Engl. Transl.), vol. 41, no. 1, p. 90].
26. Gueret, C., Daroux, M., and Billaud, F., *Chem. Eng. Sci.*, 1997, vol. 52, no. 5, p. 815.
27. Baker, R.T.K., *Carbon*, 1989, vol. 27, no. 3, p. 315.
28. Lacerda, R.G., Teh, A.S., Yang, M.H., Teo, K.B.K., Rupesinghe, N.L., Dalal, S.H., Koziol, K.K.K., Roy, D., Amaratunga, G.A.J., Milne, W.I., Chhowalla, M., Hasko, D.G., Wyczisk, F., and Legagneux, P., *Appl. Phys. Lett.*, 2004, vol. 84, no. 2, p. 269.